Article | Received 12 February 2026; Revised 11 May 2026; Accepted 13 June 2026; Published 2 September 2026
https://doi.org/10.55092/rse20260006

Formation mechanism and particle size distribution optimization of large fly ash particles

Jiajun Du[1], Zixiu Jia[2,3], Zhongcan Yang[2,3], Yonggang Zhao[1], Chaoyang Zhu[4], Yang Bai[1], Wen Tan[4], Xilai Zhang[2,3], Jiamin Gao[5] and Peipin Wang[6,*]

[1] Technical Support Center, Guoyuan Power (Shendong Power) Co., Ltd., Xi'an, China
[2] Xi'an Thermal Power Research Institute Co., Ltd., Xi'an, China
[3] Shaanxi Provincial Engineering Technology Research Center for Environmental Protection of Coal-fired Power Plant Boilers, Xi'an, China
[4] State Grid Energy Hefeng Coal and Power Co., Ltd., Tacheng, China
[5] Xi'an Yitong Thermal Engineering Technical Services Co., Ltd., Xi'an, China
[6] School of Mechanical and Power Engineering, Zhengzhou University, Zhengzhou, China

* Correspondence author; E-mail: wppyhh@zzu.edu.cn.

Highlights:

- Coarse fly ash correlates with sulfur, pyrite, ignition temperature and burnout.
- Molten (Fe–O–S) eutectics adhere to ash particles, forming larger agglomerates.
- Measures cut > 45 μm ash from 52.2% to 36.0%, meeting Grade III standard, no retrofit.

Abstract: To address the issue of coarse fly ash particles resulting from co-firing inferior coal in utility boilers—which impairs resource utilization and economic performance of power plants—this study conducts laboratory-scale investigations on coal combustion characteristics and fly ash particle size distribution, alongside field tests on coal blending and combustion optimization for a 330 MW unit. The research is approached from the perspective of reducing technical costs while avoiding large-scale equipment modifications. The formation mechanism of large fly ash particles is systematically analyzed, and optimization strategies are proposed. Laboratory results demonstrate that the proportion of coarse fly ash particles exhibits significant correlations with sulfur and pyrite content in coal, fuel ignition temperature, combustion burnout difficulty, and slagging propensity. Higher sulfur content, elevated ignition temperatures (> 680 °C), and lower burnout rates correspond to increased proportions of particles larger than 45 μm (reaching up to 38.5%). The fundamental mechanism involves the adhesion of molten (Fe–O–S) eutectics—formed through the oxidation of iron and sulfur—to other particles, thereby generating larger agglomerates. Field tests indicate that by increasing the as-fired coal calorific value to 4191 kcal/kg, reducing sulfur content to 1.04%, decreasing the proportion of low-reactivity coal, and optimizing combustion parameters (oxygen concentration at 3.8%, reduced primary air flow, and appropriately increased over-fire air opening), the proportion of fly ash particles exceeding 45 μm decreased from 52.2% to 36.0%, meeting the utilization standard for Grade III fly ash. This research achieves the technical objective of reducing coarse fly ash proportions through optimization measures without equipment modification, providing an economically viable solution for the resource utilization of fly ash from utility boilers.

Keywords: fly ash particle size; cause of large particles; blended coal combustion; combustion optimization; resource utilization

1. Introduction

Fly ash is one of the industrial wastes with the largest output in the world at present. In 2024, coal-fired power plants in China generated 780 million tons of fly ash, with an average comprehensive utilization rate of 80.8%, among which the utilization in the construction industry accounted for 79.9%, and the rest was involved in agriculture, chemical industry, metallurgy and other fields [1]. As a typical industrial solid waste, its comprehensive utilization has become a crucial issue for global circular economy and low-carbon transition. Many countries have incorporated fly ash resource utilization into national green industry strategies, issued mandatory mixing ratios and emission standards, and promoted the transformation of traditional stockpiling and disposal methods to high-value-added applications [2].

The traditional stockpiling and landfilling methods not only occupy a large amount of land resources (with an average land occupation of about 0.8 mu per 10,000 tons of fly ash) but also trigger ecological and environmental risks such as dust pollution and heavy metal leaching, posing multiple threats to the surrounding soil, water bodies and atmospheric environment [3]. Against this background, coupled with the promotion of the "dual carbon" goals and policies for the comprehensive utilization of bulk solid wastes, the resource utilization of fly ash has become an urgent requirement to alleviate environmental pressure and practice the circular economy [4].

The fineness of fly ash has become an important factor limiting its resource utilization [5]. As coal-fired power plants gradually transition to peaking regulation power sources, prolonged deep peak shaving leads to decreased unit efficiency, higher coal consumption rates for power generation, and enormous operational pressures. This compels them to seek lower-priced economical coal types.

With the co-firing of low-quality coal, fuel supply conditions for power plants become more complex. For instance, low-quality coal includes many types with low calorific value, high ash content, and high sulfur content, some containing substantial amounts of gangue. The calorific values of these fuels are generally lower than those of currently used coal. To maintain the boiler's load-carrying capacity, the overall fuel input quantity must increase, introducing large amounts of impurities into the furnace and creating a more severe combustion environment. These factors collectively affect fly ash properties, with some power plants experiencing an increase in the proportion of ash particles > 45 μm in their ash silos and coarser ash particle sizes. For example, a power plant in Ningxia [6] faced sales difficulties due to coarse fly ash particles, while a power plant in Brazil [7] experienced frequent wear and tube ruptures caused by excessive large particles, threatening operational safety, stability, and economic performance.

When fly ash particles flow in the boiler flue, they cause erosion and wear to the heating surfaces of the boiler. This wear is mainly induced by the friction and collision between fly ash particles and the metal tube walls of heating surfaces, with approximately 20% of fly ash particles contributing to such erosion and wear [8]. It is generally recognized that for particles with a size below 200 μm, the erosion effect on materials increases with the growing particle size [9,10]. The increase in fly ash particle size intensifies the erosion and wear of heating surfaces and catalysts. Long-term scouring by particles carried in flue gas can lead to thinning and even bursting of heating surface tubes, as well as catalyst abrasion [11], thereby threatening the safe operation of units.

To address the wear caused by large fly ash particles, conventional measures involve installing anti-wear components (e.g., anti-wear beams [12], anti-wear tiles [13]) and applying wear-resistant materials (e.g., refractory materials [14] and wear-resistant coatings [15]). However, all these methods require periodic reconstruction of anti-wear layers and replacement of anti-wear components. In some cases, unexpected detachment of components or coatings results in failure to achieve the desired anti-wear effect.

In response to wear induced by large fly ash particles, scholars at home and abroad have proposed large particle pre-removal technologies, including high-temperature electrostatic precipitation [3], large particle interception nets [16], and high-temperature cyclone separators similar to the material return devices of circulating fluidized beds. These technologies aim to reduce the particle size of subsequent fly ash and prevent wear on heating surfaces and catalysts by pre-separating large particles before dust collection. Nevertheless, high-temperature electrostatic precipitators and cyclone separators significantly increase the flue gas pressure drop along the path, and there are currently no mature application cases in large-scale pulverized coal boilers. Large particle interception nets have been applied in numerous projects, but they exhibit excellent removal efficiency only for particles larger than 4000 μm, while their removal effect on particles smaller than 4000 μm is limited [7].

The aforementioned technologies either achieve anti-wear effects through passive protection or remove coarse particles to a certain extent via equipment modification. All of them require equipment reconstruction, leading to substantial investment. In addition, some technologies lack application cases in large-scale units, resulting in high application risks. At present, the technology of systematically reducing the proportion of irregular large particles in fly ash from coal-fired power plants through optimization methods without equipment modification remains a blank in China. This paper conducts a study on optimization methods for reducing the proportion of large fly ash particles. The causes of large fly ash particles are analyzed in the laboratory, and the influencing factors affecting fly ash particle formation are explored. Based on the research results, an analysis of the coal combustion structure and fly ash characteristics of a 330 MW unit is performed. Drawing on the laboratory research conclusions, the particle size of fly ash is controlled and optimized through equipment optimization, coal blending and co-combustion, and other means to improve the quality of fly ash.

2. Methods

2.1. Experimental methods

Industrial analysis, elemental analysis, calorific value measurement, ash composition analysis, and pyrite content determination were conducted on six single coals selected from available fuel sources (1 high-, 3 medium-, 2 low-calorific-value). These coals cover high/medium/low calorific value, high/low sulfur, high/low volatile matter, and varied combustibility. Such selection ensures comprehensive quantitative correlation with coarse fly ash formation. Single coal samples are used to avoid blending interference, enabling accurate identification of agglomeration factors and theoretical support for field optimization.

In terms of fly ash particle size distribution and composition analysis, a one-dimensional furnace test was performed on the aforementioned boiler to investigate its ignition, burnout, and slagging characteristics. Fly ash samples were collected, and X-ray fluorescence (XRF) spectrometry and energy-dispersive X-ray spectroscopy combined with scanning electron microscopy (EDS-SEM) were employed to analyze the elemental contents of fly ash with different particle sizes, thereby clarifying the formation mechanism of coarse fly ash particles.

However, this apparatus operates under one-dimensional flow, isothermal sections, and ideal conditions; it cannot fully reproduce the three-dimensional turbulence, temperature field gradients, non-uniform gas-solid mixing, large-scale burner flow characteristics, and complex heat transfer processes within a 330 MW unit boiler furnace. Consequently, certain discrepancies exist in local temperature distribution and actual particle residence time compared with field conditions, constituting the primary limitation when scaling up from laboratory apparatus to engineering application. Therefore, the test conclusions from this laboratory apparatus require further scale-up validation on industrial furnaces.

2.2. Experimental apparatus

The ignition temperature test rig was used to measure the ignition temperature of the mixed coal samples, while the one-dimensional flame furnace test rig was adopted to determine the burnout rate [17] and slagging characteristics [18] of the mixed samples. The ignition furnace and one-dimensional flame furnace test rig are illustrated in Figure 1.

Figure 1. Ignition furnace and one-dimensional flame furnace test rig.

A schematic diagram of the ignition temperature test rig is shown in Figure 2. The rig consists of a furnace body, an air supply fan, an induced draft fan, a powder feeder, a dust collector, and a control system, and is equipped with monitoring modules for air flow, pressure, and temperature.

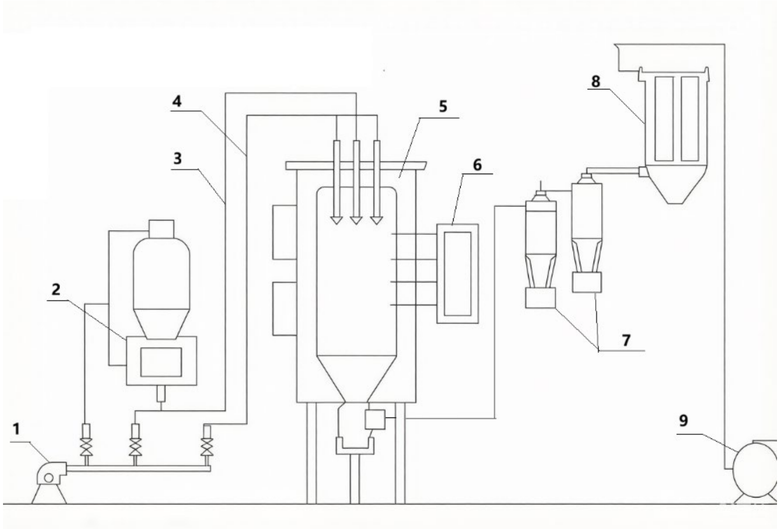

1. Air Supply Fan; 2. Powder Feeder; 3. Primary Air Duct; 4. Secondary Air Duct; 5. Furnace Body; 6. Recorder; 7. Cyclone Separator; 8. Baghouse Dust Collector; 9. Induced Draft Fan.

Figure 2. Schematic diagram of the ignition temperature test furnace.

The combustion test platform of the one-dimensional flame furnace comprises a feeding device, air supply and induced draft device, furnace body, dust collector, control system, and other components. The test platform and its schematic diagram are shown in Figure 3.

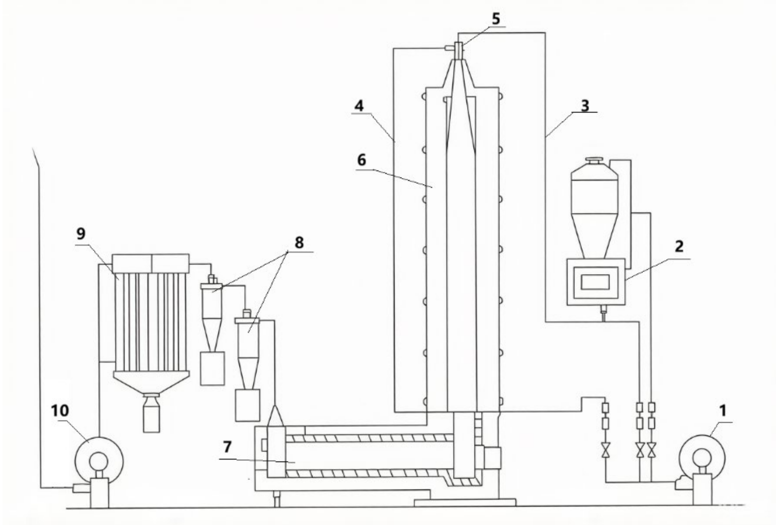

1. Air Supply Fan; 2. Powder Feeder; 3. Primary Air Duct; 4. Secondary Air Duct; 5. Burner; 6. Furnace Body; 7. Horizontal Flue; 8. Cyclone Separator; 9. Baghouse Dust Collector; 10. Induced Draft Fan.

Figure 3. Xi'an Thermal Power Research Institute Co., Ltd. (TPRI) pulverized coal combustion one-dimensional flame furnace test rig.

The one-dimensional flame furnace allows precise control of combustion temperature, atmosphere, coal particle residence time, and air distribution. It can steadily reproduce the ignition, burnout, slagging, and ash formation characteristics of pulverized coal. As a standard laboratory apparatus for coal combustion research, it can effectively simulate the core combustion environment of large-scale boilers, thus demonstrating good rationality.

3. Results

3.1. Fuel analysis results

The proximate analysis, ultimate analysis, calorific value, and coal ash composition of the fuel are presented in Table 1 and Table 2. Detailed coal quality data are provided in Supplementary Table S1. The laboratory tests were conducted in accordance with current standards, including GB/T 212-2008 Proximate analysis of coal, DL/T 568-2013 Test methods for instrumental determination of carbon, hydrogen, and nitrogen in laboratory samples of coal, GB/T 213-2008 Determination of calorific value of coal, and GB/T 1574-2007 Test method for analysis of coal ash.

Table 1. Coal quality data of furnace-fed coal.

Test Item	Total Moisture M_t/%	As-Received Basis Ash A_{ar}/%	Dry Ash-Free Basis Volatile Matter V_{daf}/%	As-Received Basis Carbon C_{ar}/%	As-Received Basis Hydrogen H_{ar}/%	As-Received Basis Nitrogen N_{ar}/%	As-Received Basis Oxygen O_{ar}/%	Total Sulfur S_t/%	As-Received Basis Net Calorific Value $Q_{net,ar}$/kcal/kg
1	6.90	53.37	45.43	27.65	2.31	0.44	8.42	0.91	2394
2	3.40	33.66	35.74	50.77	3.32	0.76	5.91	2.18	4644
3	2.90	30.99	35.63	53.31	3.49	0.79	5.21	3.31	4912
4	16.90	33.33	42.02	37.13	2.53	0.40	8.80	0.91	3158
5	4.30	23.10	11.69	66.10	2.64	0.93	0.98	1.95	5824
6	15.90	12.12	34.85	59.99	3.27	0.60	7.55	0.57	5253

Table 2. Coal ash composition of furnace-fed coal.

Coal Sample No.	Silicon Dioxide in Coal Ash (SiO_2/%)	Aluminum Oxide in Coal Ash (Al_2O_3/%)	Iron (III) Oxide in Coal Ash (Fe_2O_3/%)	Calcium Oxide in Coal Ash (CaO/%)	Magnesium Oxide in Coal Ash (MgO/%)	Sodium Oxide in Coal Ash (Na_2O/%)	Potassium Oxide in Coal Ash (K_2O/%)	Titanium Dioxide in Coal Ash (TiO_2/%)	Sulfur Trioxide in Coal Ash (SO_3/%)	Manganese Dioxide in Coal Ash (MnO_2/%)	Phosphorus Pentoxide in Coal Ash (P_2O_5/%)	Pyritic Sulfur in Coal Ash ($S_{p,ad}$/%)
1	52.23	34.71	6.40	1.48	0.36	0.80	0.73	1.27	1.38	0.019	0.151	0.30
2	45.33	33.16	11.23	4.38	0.50	0.74	0.68	1.17	2.25	0.058	0.214	0.74
3	40.56	34.02	14.70	4.33	0.40	0.59	0.54	1.29	2.60	0.048	0.209	0.82
4	59.41	18.28	11.27	3.19	1.39	0.64	2.58	1.23	0.85	0.245	0.166	0.63
5	52.95	25.96	8.64	6.17	0.74	0.33	0.73	1.26	2.10	0.075	0.596	1.01
6	53.66	16.35	9.69	10.86	0.92	0.83	1.40	1.19	3.85	0.164	0.699	0.56

3.2. Experimental procedures and results

During the experiment, the fineness of the 6 coal samples was ground to an R90 of 17%–18%, and the operating oxygen content was controlled at 3.5%. The fly ash collected from the cyclone separator and horizontal flue of the one-dimensional furnace was subjected to screening. The screening results of various coal types are presented in Figure 4 and Supplementary Table S2. The proportions of fly ash particles with sizes below 45 μm were 76.90%, 70.30%, 61.51%, 91.64%, 62.63% and 81.54%, respectively. In descending order of the proportion of coarse fly ash particles, the ranking of coal types was as follows: Coal 3 > Coal 5 > Coal 2 > Coal 1 > Coal 6 > Coal 4.

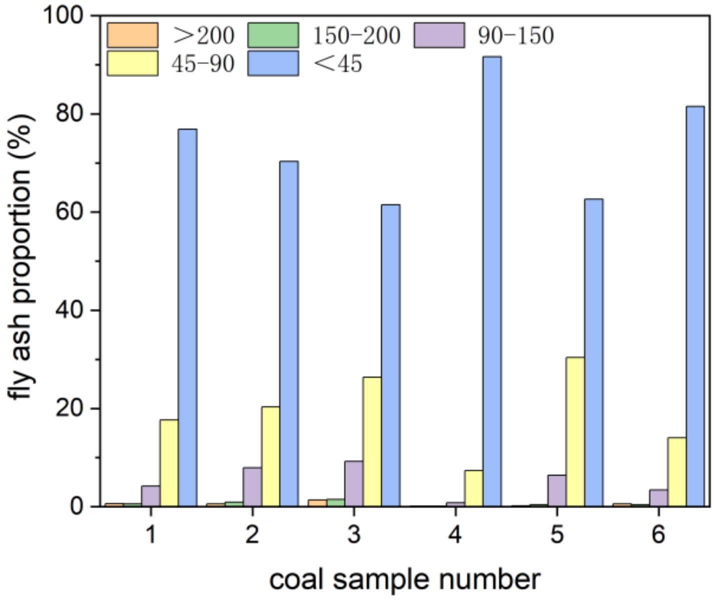

Figure 4. Particle size distribution of combustion products from different coal samples.

Figure 5 shows the relationship between the proportion of fly ash particles smaller than 45 μm and the contents of total sulfur as well as pyritic sulfur (Supplementary Table S3). As indicated in the figure, the higher the contents of total sulfur and pyritic sulfur, the lower the proportion of fly ash particles with sizes below 45 μm, and the more large particles existed in the fly ash, showing a strong correlation.

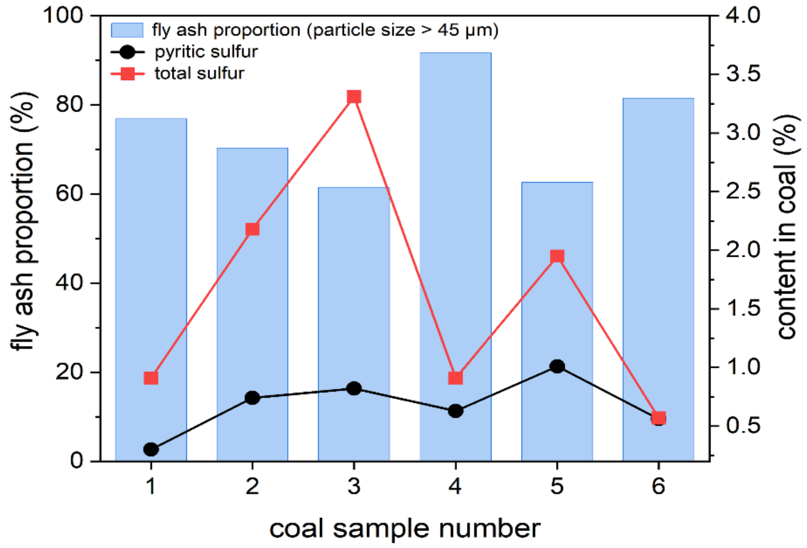

Figure 5. Correlation between fly ash particle size and sulfur content in fuel.

It is worth noting that total sulfur comprises organic sulfur, sulfate sulfur, and pyritic sulfur (FeS_2). As indicated in Figure 5, pyritic sulfur plays a promoting role in fly ash particle agglomeration: it oxidizes rapidly at relatively low temperatures and directly supplies both iron and sulfur for the formation of the Fe–O–S eutectic melt. Consequently, the correlation observed between total sulfur and fly ash particle size distribution is partially attributable to its pyritic sulfur fraction.

Figure 6 depicts the variation in ignition temperature for different coal sample numbers. The ignition temperatures of the six coal samples ranged from 540 °C to 760 °C (Table 3 and Supplementary Table S4). Samples 1, 2, and 5 were classified as difficult to ignite; Sample 3 was moderately ignitable; Sample 6 was easy to ignite; and Sample 4 was extremely easy to ignite. Although Coal Samples 1, 2, and 3 exhibited relatively high volatile matter contents, their ignition temperatures were higher than that of Sample 6 due to the flame-retardant effect of high ash content.

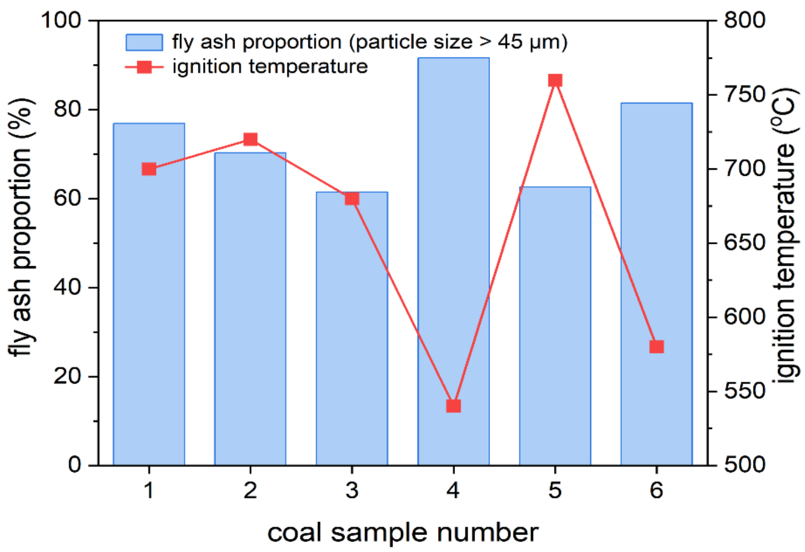

Figure 6. Correlation between fly ash particle size and fuel ignition temperature.

Table 3. Ignition temperatures of samples.

Coal Sample No.	Ignition Temperature IT	Ignition Grade
1	700	Difficult
2	720	Difficult
3	680	Middle
4	540	Extremely Easy
5	760	Difficult
6	580	Easy

In terms of the content of large fly ash particles, under the condition of the same pulverized coal fineness, the coarser particle sizes of Samples 1, 2, 3 and 5 were significantly correlated with their low combustion reactivity.

3.3. Microscopic morphology and elemental analysis of particles with different sizes

Table 4 presents the morphology of fly ash samples derived from Coal Sample 3. For particles larger than 200 μm, most exhibited an irregular morphology with obvious signs of particle agglomeration and sintering. Around the molten matrix in the center of large particles, a large number of spherical or irregular small particles adhered to the surface. In contrast, particles smaller than 45 μm mostly existed as discrete spherical particles, without any particle agglomeration or adhesion.

Table 4. Analysis of fly ash samples from coal Sample 3.

Fly Ash Particle Size	Morphology at 2000× Magnification	Morphology at 20000× Magnification	Morphology at 40000× Magnification
> 200 μm	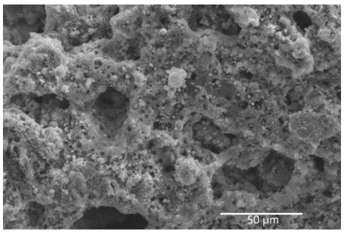	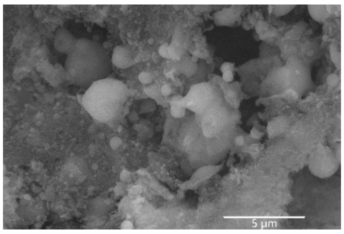	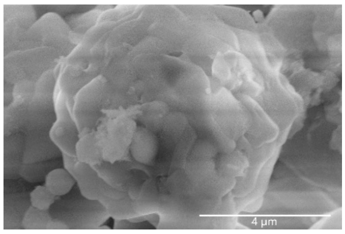
< 45 μm	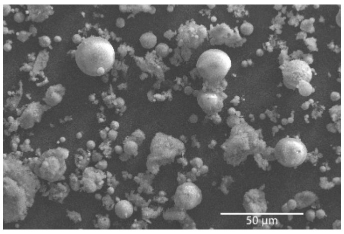	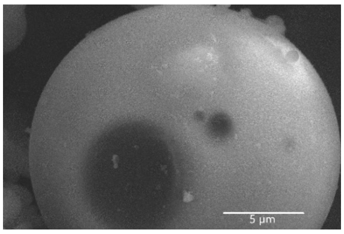	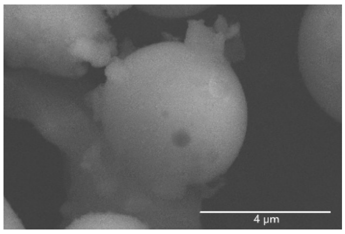

Energy dispersive spectroscopy (EDS) point analyses were conducted on the surfaces of coarse ash particles (> 200 μm), and the detection results are listed in Table 5.

Table 5. EDS detection results of ash particle surfaces (> 200 μm)/%.

Element	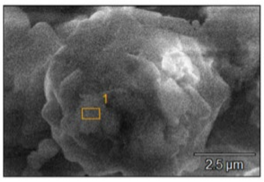	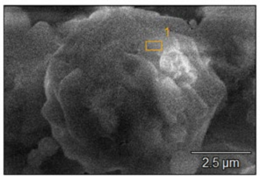	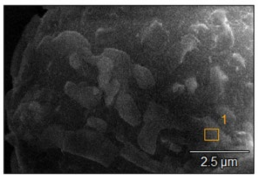	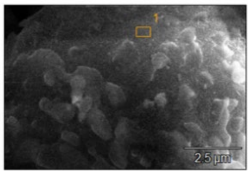
C	6.02	8.60	3.28	3.78
O	54.42	50.79	53.55	51.21
Na	0.62	0.61	2.34	2.58
Mg	0.09	0.08	1.10	1.45
Al	5.56	1.42	3.54	5.89
Si	6.12	2.12	8.56	13.71
S	5.77	5.92	3.95	ND
K	0.37	0.47	ND	0.36
Ca	7.82	8.54	8.15	7.59
Ti	2.76	0.90	6.33	1.64
Mn	1.24	2.39	ND	ND
Fe	9.19	18.16	9.21	11.80

The EDS detection results of fine ash particles (< 45 μm) are listed in Table 6.

Table 6. EDS detection results of ash particles (< 45 μm)/%.

Element	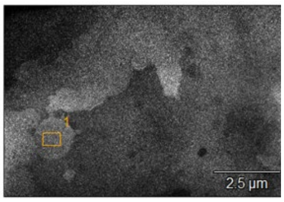	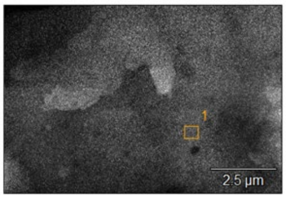	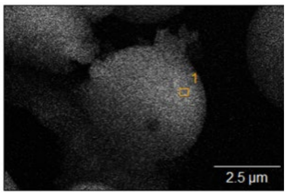	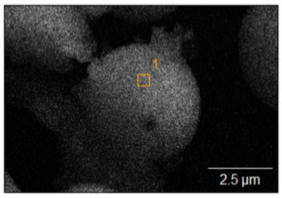
C	11.32	1.69	14.37	6.55
O	51.95	50.41	46.00	52.60
Na	0.37	ND	ND	ND
Mg	0.14	ND	ND	ND
Al	14.95	23.27	13.66	15.10
Si	15.51	23.85	14.53	15.63
S	0.19	ND	ND	ND
K	0.28	0.40	ND	ND
Ca	2.31	0.37	9.83	9.71
Ti	0.94	ND	0.70	0.41
Mn	0.09	ND	ND	ND
Fe	1.95	ND	0.92	ND

ND: Not Detected (below the detection limit of the EDS instrument).

Energy dispersive spectroscopy (EDS) analyses were conducted on fly ash particles with distinct particle sizes. The cross marks illustrated on the left-hand side of Table 4 correspond to the EDS detection locations. As revealed by the analytical results, the contents of sulfur (S) and iron (Fe) in large particles are substantially higher than those in small particles, whereas the contents of silicon (Si) and aluminum (Al) are relatively lower in large particles. For the majority of large particles, the Fe content in the smooth molten regions is higher than that in the surface-adhered substances. A considerable number of irregularly shaped small particles adhere to the surfaces of large particles, and significant compositional discrepancies exist between the refractory sharp segments and the molten smooth regions of large particles.

During the combustion and oxidation processes, Fe and S elements can form a molten intermediate (Fe–O–S) with extremely strong adhesiveness at approximately 1300 K (1027 °C), which is generally designated as the iron-oxygen-sulfur eutectic [19]. The highly viscous Fe–O–S molten eutectic phase exhibits strong adhesion ability. It can continuously bond and encapsulate surrounding fine ash particles, and finally form large particles through agglomeration and sintering. EDS results confirm that the contents of Fe and S in particles larger than 200 μm are much higher than those in particles smaller than 45 μm, which directly supports the above mechanism. The presence of this eutectic significantly enhances the probabilities of agglomeration, adhesion, and coalescence among ash particles, thereby elevating the likelihood of small particles transforming into large particles.

3.4. Optimization test of full-scale boiler

The fly ash particle size of a 330 MW unit coarsened in 2022, which adversely affected the sales of fly ash products.

Based on the results of laboratory tests, targeted adjustments and optimizations were implemented under the 220 MW load (a commonly applied operational condition for the unit). During the adjustment process, the boiler evaporation capacity was kept constant, and fly ash samples were collected from both sides of the flue under different operating conditions.

3.5. Adjustment of operational parameters

The boiler operating oxygen concentration was adjusted to 3.1%, 3.6%, and 4.1%, respectively. The fly ash particle sizes on the left and right sides were measured under each condition. The unit operating parameters before adjustment are shown in Table 7, and the test results after oxygen adjustment are presented in Figure 7 and Supplementary Table S5.

Table 7. Parameters before oxygen adjustment.

Item	Unit	Condition
Operating O_2	%	3.1
Total coal flow	t/h	148
Calorific value of coal	kcal/kg	3573
Sulfur content of coal	%	0.97
Separator speed	rpm	5
Burn-out damper opening	%	25
Primary air flow (A/B/C/D mills)	t/h	47/52/46/40
Proportion of Fly Ash Particles > 45 μm	%	52.2

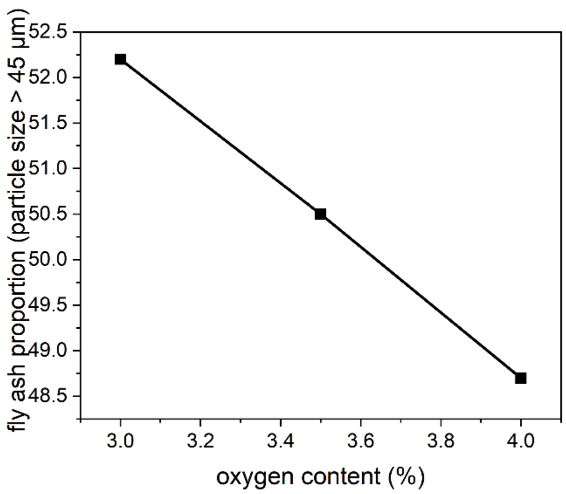

Figure 7. Relationship between fly ash particle size and excess oxygen concentration.

The results indicate that the higher the excess oxygen concentration, the smaller the average particle size of fly ash. A higher operational oxygen concentration facilitates accelerating the combustion reaction rate of pulverized coal, promotes the complete oxidation of iron sulfide, and thus reduces the formation of large particles.

The primary air flow of the boiler was adjusted. The unit operating parameters before adjustment are shown in Table 8, and the test results after primary air adjustment are presented in Figure 8. The primary air flow rates of the four mills were reduced from 48/52/45/40 t/h to 44/45/40/35 t/h, a reduction of approximately 8%, and the fly ash particle size decreased accordingly.

Table 8. Parameters before primary air adjustment.

Item	Unit	Condition
Operating O_2	%	4.1
Total coal flow	t/h	144
Calorific value of coal	kcal/kg	3722
Sulfur content of coal	%	1.41
Separator speed	rpm	20
Burn-out damper opening	%	25
Primary air flow (A/B/C/D mills)	t/h	48/52/45/40
Proportion of Fly Ash Particles > 45 μm	%	65.8

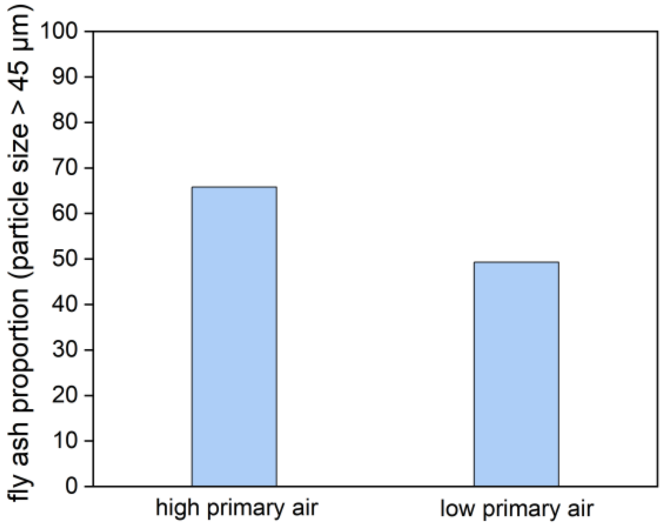

Figure 8. Relationship between fly ash particle size and primary air flow rate.

It is analyzed that the reduction in primary air flow lowers the required ignition heat, which advances the ignition and combustion of the coal-air flow and improves the coal burnout rate. Meanwhile, the oxidation rate of total sulfur is accelerated, suppressing the formation of Fe–O–S intermediates. In addition, the decrease in furnace exit gas temperature helps reduce the viscosity of low-melting eutectic phases. Overall, these changes are conducive to inhibiting the formation of coarse fly ash particles.

At a boiler load of 220 MW, the opening of the over-fire air (OFA) damper was adjusted to 25%, 50%, and 80%, respectively. The effects of OFA damper variation on operating parameters such as fly ash particle size and boiler efficiency were investigated. The operating parameters before OFA damper adjustment are listed in Table 9, and the experimental results are presented in Figure 9.

Table 9. Parameters before OFA adjustment.

Item	Unit	Condition
Operating O_2	%	3.7
Total coal flow	t/h	153
Calorific value of coal	kcal/kg	3766
Sulfur content of coal	%	1.27
Separator speed	rpm	5
Burn-out damper opening	%	25
Primary air flow (A/B/C/D mills)	t/h	48/52/45/40
Proportion of Fly Ash Particles > 45 μm	%	62.2

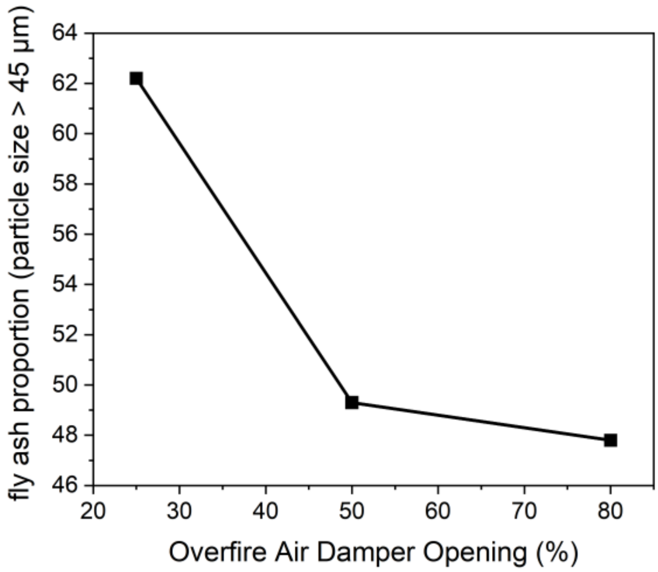

Figure 9. Relationship between fly ash particle size and OFA damper opening.

A relatively high OFA flow rate can effectively reduce the particle size of fly ash. In the OFA zone, the sufficient oxidation of unburnt sulfur is achieved, which inhibits the formation of Fe–O–S intermediate eutectics and thus mitigates the generation of large fly ash particles.

The variation of oxygen concentration directly influences the pulverized coal combustion reaction rate, furnace temperature level, and oxidation degree of mineral elements [9]. As shown in Figure 7, when the oxygen concentration increases from 3.1% to 4.1%, the proportion of fly ash particles larger than 45 μm shows a continuous decreasing trend. The elevated oxygen concentration strengthens the oxygen supply in the high-temperature combustion zone, which raises the furnace temperature and promotes the full combustion of pulverized coal particles [12]. Meanwhile, the enhanced oxidation atmosphere accelerates the sufficient oxidation of Fe and S elements in coal ash, which inhibits the formation of molten Fe–O–S eutectics with strong viscosity [19].

Under higher oxygen concentration, the fly ash surface morphology changes significantly: large particles with obvious agglomeration and melting adhesion are reduced, while small spherical particles with smooth surfaces increase [4]. This is because the sufficient oxidation environment reduces the production of low-melting eutectic substances, weakens the adhesion between fine ash particles, and suppresses the physical process of particle agglomeration and sintering [12]. Therefore, oxygen concentration affects the fly ash particle size distribution by controlling the combustion temperature field, the surface morphology of ash particles, and the chemical reaction path of Fe–O–S eutectic formation.

3.6. Adjustment of feed coal quality

Laboratory test results show that the formation of coarse fly ash particles is closely related to total sulfur, pyritic sulfur content, as well as coal combustion and burnout characteristics. Therefore, during field tests, coal type and calorific value were varied to investigate the effect of coal quality on fly ash particle size.

Coal blending was carried out using available on-site coal samples. The blending schemes were designed with gradients around two key parameters, namely calorific value and total sulfur content, to achieve controllable variables and clear comparisons. Sulfur content was taken as the primary distinguishing indicator. Fe in ash is difficult to detect online continuously, whereas sulfur content is strongly correlated with Fe–O–S eutectic formation and particle agglomeration and can be easily measured and controlled. When calorific values are similar, samples are distinguished by sulfur content to compare its effect on coarse particle formation. When sulfur contents are similar, samples are distinguished by calorific value to compare the effects of coal reactivity and combustion intensity.

The operating parameters before coal sample adjustment are shown in Table 10 and the coal blending ratio adjustment scheme is presented in Table 11.

Table 10. Operating parameters before coal sample adjustment.

Item	Unit	Condition
Operating O_2	%	3.6
Total coal flow	t/h	140.4
Calorific value of coal	kcal/kg	3573
Sulfur content of coal	%	0.97
Separator speed	rpm	5
Burn-out damper opening	%	25
Primary air flow (A/B/C/D mills)	t/h	48/52/45/40
Proportion of Fly Ash Particles > 45 μm	%	50.5

Table 11. Composition of blended coal in co-firing tests.

Blending Scheme	Coal Sample 1 (%)	Coal Sample 2 (%)	Coal Sample 4 (%)	Coal Sample 5 (%)	Coal Sample 6 (%)	Calorific Value of Feed Coal (kcal/kg)	Sulfur Content of Feed Coal (%)	Proportion of Fly Ash Particles > 45 μm
1	37.5	25.0	25.0	12.5	0.0	3577	0.97	50.5
2	25.0	0.0	50.0	25.0	0.0	3770	1.27	49.3
3	25.0	0.0	37.5	25.0	12.5	3726	1.41	55.2
4	25.0	25.0	0.0	25.0	25.0	4191	1.04	45.0
5	0.0	0.0	0.0	50.0	50.0	4950	1.25	55.0

To explore the influence of coal quality variation on fly ash particle size, coal blending tests were carried out, taking the calorific value and total sulfur content of furnace-feed coal as the main control variables. The results are analyzed as follows:

With the increase of coal calorific value from 3577 kcal/kg to 4950 kcal/kg, the blending scheme 4 with a calorific value of 4191 kcal/kg presents the lowest proportion of coarse fly ash particles at 44.7%. This indicates that higher combustion intensity and burnout rate can reduce the generation of unburned carbon and molten agglomerated particles. It is noteworthy that blending scheme 5 has the highest calorific value of 4950 kcal/kg, while its coarse fly ash particle proportion reaches 54.8%, which is higher than that of scheme 4. This is attributed to the simultaneous increase of sulfur content (1.25% *vs.* 1.04%), which offsets the positive effect brought by high calorific value. Meanwhile, scheme 5 has a similar sulfur content but higher calorific value compared with scheme 2, yet higher calorific value shows a negative effect in this case. This conclusion is consistent with the single-coal test results in laboratory tests: blending coal with low combustion reactivity will increase the proportion of coarse fly ash particles.

The increase of sulfur content promotes the formation of low-melting Fe–O–S eutectic phases in coal ash, enhances the adhesion of ash particles, and aggravates particle agglomeration and sintering, thereby increasing the proportion of coarse particles. An obvious positive correlation is observed in the test results: when the sulfur content rises from 0.97% (scheme 1) to 1.41% (scheme 3), the proportion of coarse fly ash particles increases from 50.5% to 55.2%. The comparison between scheme 2 (1.27%

sulfur) and scheme 4 (1.04% sulfur) further verifies this trend. Under similar sulfur content, higher calorific value corresponds to a lower proportion of coarse fly ash particles, which confirms the coupling effect of calorific value and sulfur content.

The combined effect of calorific value and sulfur content determines the final fly ash particle size distribution:

Comparison of scheme 1 and scheme 4: with similar sulfur content, the positive effect of increased calorific value is dominant;

Comparison of scheme 2 and scheme 3: the negative effect of increased sulfur content dominates, leading to a significant increase in fly ash particle size;

Comparison of scheme 3 and scheme 4: the simultaneous improvement of calorific value and reduction of sulfur content achieves the optimal control of fly ash particle size.

Compared with scheme 4, blending low combustion reactivity coal in scheme 5 increases the proportion of coarse fly ash particles.

In general, sulfur content is the key promoting factor for the formation of coarse fly ash particles, while appropriately high calorific value can effectively offset its adverse impact. Therefore, the optimal coal blending strategy should give priority to controlling the sulfur content of furnace-feed coal and maintain a reasonable high calorific value, so as to minimize the formation of coarse fly ash particles.

3.7. Operation of optimal parameters

The baseline operating parameters are shown in Table 7. By adjusting the coal blending ratio to Scheme 4, increasing the operating oxygen content to 3.8%, setting the overfire air opening to 50%, and reducing the primary air flow by approximately 8%, the proportion of fly ash particles larger than 45 μm decreased significantly from 52.2% to 36%. The operating performance before and after adjustment is presented in Table 12.

After optimization, the dry flue gas heat loss decreased from 6.21% to 5.96% relative to the baseline condition. Although the elevated oxygen content increased the dry flue gas volume, the corrected exhaust gas temperature dropped from 153.2 °C to 144.4 °C, which was sufficient to offset this effect.

Table 12. System parameters and effects after optimization.

Item Name	Unit	Baseline Condition	After Adjustment
Unit Load	MW	220	220
Main Steam Flow	t/h	734	715
Fuel Consumption	t/h	148.2	119.6
Operating Oxygen Content	%	3.1	3.8
Carbon Content in Fly Ash	%	3.02	1.42
CO Emission	ppm	0	0
Unburned Carbon Loss	%	2.60	0.88
Heat Loss Caused by CO	%	0.00	0.00
Heat Loss with Dry Flue Gas	%	6.21	5.96
Boiler Efficiency	%	90.04	92.10
NOx Emission Concentration	mg/m3	856	700
Fly Ash Particle Size	%	52.2	36.0

4. Conclusion

Laboratory studies in this paper show that fly ash particle size is closely related to the total sulfur and pyrite sulfur content in coal, fuel ignition temperature, difficulty in burnout, and slagging tendency. The primary cause of coarse fly ash formation is the high total sulfur and pyritic sulfur contents of the coal. When coal reactivity is low and combustion intensity is insufficient, the oxidation of Fe- and S-containing species is slowed, promoting the formation of molten Fe–O–S eutectics in the horizontal flue temperature range.

By combining laboratory mechanistic investigations with field-test verification, the optimization strategies proposed in this study demonstrate strong potential for engineering application and long-term operational benefits. By increasing the calorific value of the coal fed into the furnace, reducing the sulfur content, reducing the blending ratio of low-reactivity coal, and optimizing combustion parameters (increasing the operating oxygen content to 3.8%, appropriately increasing the over-fire air, and reducing the primary air under 220 MW load), the proportion of fly ash particles larger than 45 μm can be reduced from 52.2% to 36.0%, meeting the Grade III fly ash utilization standard. At the same time, it achieves the coordinated optimization of boiler efficiency, NO_x emissions, unburned carbon content in fly ash and other indicators, realizing the synchronous improvement of fly ash quality and boiler operation economy.

Combining laboratory mechanism research and on-site test verification, the optimization strategies proposed in this paper have strong engineering scalability and long-term operational benefits. Aiming at the core Fe–O–S eutectic mechanism of coarse fly ash particle formation, the adopted measures such as coal blending optimization, oxygen concentration adjustment, and air staging are not only applicable to the 330 MW unit in this study, but also universally applicable to other domestic power plant boilers burning medium-high sulfur coal, anthracite, and co-firing biomass and solid waste, and can be directly used for reference in fly ash particle size optimization of similar units; Long-term implementation of these optimization measures can also reduce the reducing atmosphere in the furnace, inhibit the formation of corrosive sulfides, thereby mitigating high-temperature corrosion, extending the service life of boiler heating surfaces and denitration catalyst equipment, reducing maintenance costs, and improving the safety and economy of unit operation; Future research will focus on quantifying the mitigation effect of optimization measures on high-temperature corrosion and further expanding the application scope of this strategy in various co-firing conditions.

Supplementary data

Supplementary tables summarizing the coal quality analysis (Supplementary Table S1), particle size distribution of fly ash from different coal samples (Supplementary Table S2), sulfur content and sulfur forms (Supplementary Table S3), ignition temperatures and ignition grades (Supplementary Table S4), and results of the full-scale boiler combustion optimization tests (Supplementary Table S5) are provided with this article.

Data availability statement

The data or datasets generated or analyzed in this study are available in Figshare at https://doi.org/10.6084/m9.figshare.32231298.

Declaration of generative AI and AI-assisted technologies

During the preparation of this manuscript, the authors used generative AI tools only to improve language and readability. Specifically, the authors used Kimi (Moonshot AI) for language polishing only. The authors take full responsibility for the content of the manuscript.

Acknowledgments

Funding: This work was funded by the Science and Technology Innovation Project of Guoyuan Power Co., Ltd., China Energy Investment Corporation, with grant number GSKJ-22-08.

Authors' contribution

Conceptualization, methodology and data curation, writing—original draft, J.D.; laboratory experiment, formal analysis and data validation, Z.J.; field test, data visualization and result analysis, Z.Y.; project administration and resource provision, Y.Z.; field test coordination and sample collection, C.Z.; mechanism analysis and data processing, Y.B.; coal quality analysis and experimental support, W.T.; supervision, methodology design and writing—review and editing, X.Z.; combustion parameter optimization and field verification, J.G.; conceptualization, supervision, funding acquisition, writing—review and editing and project administration, P.W. All authors have read and agreed to the published version of the manuscript.

Conflicts of interest

Jiajun Du, Yonggang Zhao, Chaoyang Zhu, Yang Bai, Wen Tan, Xilai Zhang, and Jiamin Gao are employees of Guoyuan Power (Shendong Power) Co., Ltd., State Grid Energy Hefeng Coal and Power Co., Ltd., and Xi'an Yitong Thermal Engineering Technical Services Co., Ltd., respectively. Zixiu Jia and Zhongcan Yang are affiliated with Xi'an Thermal Power Research Institute Co., Ltd. The authors declare that these affiliations do not influence the design, analysis, interpretation, or presentation of the results reported in this manuscript.

References

[1] National Energy Administration. National Energy Administration releases 2024 statistical data on China's electric power industry (In Chinese). 2025. Available: http://www.nea.gov.cn (accessed on 21 January 2025).

[2] GEPResearch. Research report on the development of China's fly ash comprehensive utilization industry. 2025. Available: http://www.gepresearch.com (accessed on 30 August 2025).

[3] Han X, Zhang P, Zheng Y, Wang J. Utilization of municipal solid waste incineration fly ash with coal fly ash/metakaolin for geopolymer composites preparation. *Constr. Build. Mater.* 2023, 403:133060.

[4] Pan J, Nie T, Hassas BV, Wen Z, Zhou C. Recovery of rare earth elements from coal fly ash by integrated physical separation and acid leaching. *Chemosphere* 2020, 248:126112.

[5] Liu Y, Wang Z, Zhao W, Hou J, Cui L, *et al*. Hierarchical porous nanosilica derived from coal gasification fly ash with excellent CO_2 adsorption performance. *Chem. Eng. J.* 2023, 455:140622.

[6] Zhao T, Li G, Zhang S, Yang H, Ni W, *et al*. Enhancement effect of biochar on the immobilization of heavy metals and anions in MSWI fly ash/bottom ash–coal fly ash-based cementitious materials: risk assessment model and mechanisms. *J. Hazard. Mater.* 2025, 497:139615.

[7] Shi Y, Jiang K, Zhang T. Cleaner extraction of alumina from coal fly ash: baking-electrolysis method. *Fuel* 2020, 273:117697.

[8] Seki T, Nakamura K, Ogawa Y, Inoue C. Leaching of As and Se from coal fly ash: fundamental study for coal fly ash recycling. *Environ. Monit. Assess.* 2021, 193(4):225.

[9] Lv B, Jiao F, Chen Z, Dong B, Fang C, *et al*. Separation of unburned carbon from coal fly ash: pre-classification in liquid–solid fluidized beds and subsequent flotation. *Process Saf. Environ. Prot.* 2022, 165:408–419.

[10] Qi X, Song G, Yang S, Yang Z, Lyu Q. Investigation of corrosion characteristics of high-sodium high-chlorine lignite during circulating fluidized bed combustion. *Energy Fuels* 2017, 31(12):13627–13638.

[11] Widjajanto T, Darmadi DB, Irawan YS, Gapsari F. Failures analysis of tube coating in Circulating Fluidized Bed (CFB) boiler. *Heliyon* 2024, 10(4):e26134.

[12] Liu T, Chen J, Li X, Wang B, Ying Z, *et al*. Recycling and resource utilization of coal fly ash: a review. *Sep. Purif. Technol.* 2025, 375:133791.

[13] Pronobis M. Harmful phenomena in modernized boilers. In *Environmentally Oriented Modernization of Power Boilers*. Amsterdam: Elsevier, 2020. pp. 213.

[14] Gao X, Zhou Q, Wang Y, Qi T, Shen L, *et al*. Coal fly ash resource utilization: structure of siloxy group of high-modulus sodium silicate solution. *Process Saf. Environ. Prot.* 2023, 171:396–404.

[15] Szymański K, Hernas A, Moskal G, Myalska H. Thermally sprayed coatings resistant to erosion and corrosion for power plant boilers—a review. *Surf. Coat. Technol.* 2015, 268:153–164.

[16] Hou H, Su L, Guo D, Xu H. Resource utilization of solid waste for the collaborative reduction of pollution and carbon emissions: case study of fly ash. *J. Clean. Prod.* 2023, 383:135449.

[17] Xing L, Li X, Cao P, Luo J, Jiang H. Stepwise extraction and utilization of silica and alumina from coal fly ash by mild hydrothermal process. *Process Saf. Environ. Prot.* 2024, 182:918–929.

[18] Yang J, Huang J, Su Y, He X, Tan H, *et al*. Eco-friendly treatment of low-calcium coal fly ash for high pozzolanic reactivity: a step towards waste utilization in sustainable building material. *J. Clean. Prod.* 2019, 238:117962.

[19] Morales Sánchez C, Pascual A, Leinen D, Luna López G, Ares Fernández JR, *et al*. Reaction mechanism and kinetic model of the transformation of iron Monosulfide thin films into pyrite films. *J. Phys. Chem. C* 2025, 129(9):4724–4737.